

# A REVIEW OF ASR MODELING APPROACHES FOR FINITE ELEMENT ANALYSES OF DAMS AND BRIDGES

Rita Esposito<sup>1\*</sup>, Max A.N. Hendriks<sup>1</sup>

<sup>1</sup>Delft University of Technology, Faculty of Civil Engineering and Geosciences, Structural Mechanics,  
The Netherlands

## Abstract

In this paper the anisotropic behavior of ASR swelling is simulated through a 1D smeared crack model. The choice of the engineering properties is discussed, in particular for the evolution of the tensile strength and the Young's modulus during the swelling. The last one is used as the main indicator for ASR-related damage. The model is hampered by the lack of experimented data available in literature. The outlook of the approach is that orthotropic stiffness degradation could be used to explain anisotropic swelling.

**Keywords:** Alkali-Silica Reaction (ASR), degradation mechanical properties, modeling, crack model.

## 1. INTRODUCTION

The concrete infrastructure of bridges, dams and other civil works may be at risk to deterioration caused by alkali-aggregate reaction. In this group of reactions the Alkali-Silica Reaction (ASR) is considered one of the most harmful processes, because it generates an expansive gel. This reaction, which begins at microstructural level, may cause serious damage with consequent loss of structural capacity; the designer must be able to assess the safety at macrostructural level. The behavior of ASR damaged concrete structures can be evaluated in two phases. The first phase concerns the description of chemical kinetic law for the gel formation and swelling phenomenon. In the second phase the interaction between gel and cement matrix is defined.

In the last 20 years various structural models have been developed and implemented in finite element codes. In early proposals the gel expansion is taken in account with a thermal equivalent approach. This method was enhanced by Léger et al. [0], who defines four coefficients to evaluate the influence of the environmental conditions.

Afterwards the coupling between chemical and mechanical aspects became a relevant topic. The first example of a chemo-mechanical model is proposed by Pietruszczak [2]. In the more advanced models a kinetic law is defined for this aim. In this type of models the concrete is considered as a porous medium formed by a solid skeleton and a gel filling the pores. The most known kinetic law is obtained from the Larive's test campaign [3]; it is used in several models to describe the dependency between the swelling and temperature. This kinetic law is adopted for the first time in the isotropic damage model proposed by Ulm et al. [4]. Ulm's model is one of the most famous ones and it is the basis of many subsequent models.

In the more recent models, the research is focused on the anisotropy aspect of the swelling, presented by Larive and Multon et al. [5]. The anisotropy is observed both in free expansion condition, named intrinsic anisotropy, and in bounded specimens, named stress-induced anisotropy or defined as "expansion transfer" concept. The majority of the models does not take in account the intrinsic anisotropy or consider a crude

---

\* Correspondence to: [r.esposito@tudelft.nl](mailto:r.esposito@tudelft.nl)

formulation. The attention is focused more on the stress-induced anisotropy. In this field modeling approaches are proposed by: Multon et al [5], Saouma and Perotti [6], Comi et al. [7] and Capra and Sallier [8]. The first three models are isotropic damage model in which the expansion is characterized with an anisotropic behavior. The last one is an orthotropic damage model.

The experimental results show also that the anisotropy could be explained with the crack formation; the direction of maximum expansion is always perpendicular to the crack alignment. In this perspective, Farage et al [9] proposed a smeared crack model.

According with this last assumption, the background of the present paper is that smeared crack model is used to evaluate the anisotropic expansion behavior. The evaluation of stiffness and strength properties as a function of the degradation degree due to ASR expansion is needed. Experimental data by Larive [3], Swamy et al. [10], Ahmed et al. [11] and Giaccio et al. [12] are analyzed and a stiffness and strength degradation model is proposed.

## 2. MODELLING APPROACHES FOR ANISOTROPY EXPANSION

The anisotropic behavior of specimens in free expansion condition was first presented by Larive [3]. She observed that the gel prefers to swell in the direction parallel to the casting direction; the expansion in this direction ranges from 1.3 to 2.8 times the expansion in the perpendicular direction.

She compared also the behavior of vertically casted cylinders and horizontally casted prisms prepared with the same mix and stored in the same condition. The expansion of cylinders and prisms perpendicular to the casting direction resulted similar, as shown in Figure 1 (a).

Tensile tests on sound concrete specimens with the same particle-size show, as well known, that the tensile strength is lower along the casting direction. This indicates that the pores distribution determines both the preferred expansion direction and the direction with the weakest tensile strength. This is also confirmed from the tendency of the cracks to orientate the expansion; in fact before cracking occurs, the swelling has an isotropic behavior. In conclusion, anisotropic cracking resulting from anisotropic strength properties influence the anisotropic expansion.

Moreover, this phenomenon is not influenced by the temperature.

The same conclusion could be used to explain the “expansion transfer” concept, presented by Multon et al. [5]. In specimens subjected to compressive loading or lateral constraining the imposed expansion is lower in the restrained direction, which matches the crack alignment (Figure 1 (b))

The modeling of the anisotropic behavior is treated with different approaches. The majority of the models available in literature are isotropic damage models in which an “anisotropic expansion” is considered.

The intrinsic anisotropy is often neglected or is take in account in a crude way.

Comi et al. [7], who adopts an isotropic damage model, defines the expansion in the casting direction equal to two times the expansion in the perpendicular direction.

According with experimental data, the “expansion transfer” concept is observed in specimens subjected to compressive load. The stress induced state orients the expansion in the free direction; moreover if the stress is high it could slow down the reaction.

Multon et al. [5] evaluate the swelling in bounded specimens through an anisotropy coefficient defined as the ratio between the expansions in the direction of the load/restrain and in the direction perpendicular to it. The coefficient depends on the stress which occurs in the load direction and from the average stress in the structure.

Saouma and Perotti [6] proposed a thermo-chemo-mechanical model in which the expansion redistribution is based on weights related to the stress tensor. The weight coefficients are defined for sixteen main stress conditions and are evaluated for a generic condition through a bilinear shape function.

Comi et al. [7] adopted an isotropic damage model based on the definition of two scalar damage variables, one for stress state in tension and the other in compression. A similar approach is defined in the orthotropic model of Capra and Sallier [8], where the damage coefficients are calculated according to the cracking probabilities.

Farage et al. [9] presented a smeared crack model in which the cracking formation influences the expansion redistribution. A ductile stress-strain relationship is used to describe the post-cracking behavior. The cracking occurs in two stages: a relatively long cohesive stage with a constant strength, following by a softening stage.

Adopting a crack model to describe the anisotropic aspects of the ASR swelling, in this paper a smeared crack model is proposed in Chapter 4. In the next Chapter, the evaluation of the stiffness and strength properties degradation is highlighted and the available experimental data are compared.

### 3. DEGRADATION OF MECHANICAL PROPERTIES: OVERVIEW OF EXPERIMENTS

The determination of the mechanical properties is crucial for a reliable analysis of structures with the ASR-affected concrete as well as for structures with sound concrete. The difference is that for the second case tested formulations are provided by codes and standards, whereas for the first case few literature information is available. Moreover, the gel's properties are also an unknown. Some test campaigns are carried out from different authors to define the variation of engineering properties in ASR-affected concretes.

The first results have been performed by Swamy et al. in 1988 [10]. They showed that: "the losses in engineering properties do not occur at the same rate or in proportion to the expansion undergone by the ASR-affected concrete" [10]. More recent information was provided by Ahmed et al. [11]. To date, this is the most complete test campaign available in literature. The degradation of stiffness and compressive strength has been also studied by Giaccio et al. [12]. Furthermore, Larive provides some information related to stiffness and strength in her thesis [3].

In Table 1 an overview of the experimental results is shown. In particular, the curing and storage condition as well the type of reactive and non-reactive aggregates are reported.

The majority of the specimens were tested in water at a temperature equal to 38°C; only the specimens tested by Swamy et al. are stored at a temperature of 23°C. All the specimens are demolded after one day.

In Table 2 an overview of the measured mechanical properties are shown. The majority of the experiments are focused on concrete degradation of Young's modulus and tensile strength; in this light the Ahmed's work is the most useful, because it provides both of them. In the paper of Giaccio et al., some information is given for the concrete behavior in compression.

In Figure 2 (a) the expansion vs. time curves are given. The maximum expansion of Larive and Giaccio's specimens are close, in the first case the maximum expansion is equal to 0.196 % in the other three cases the maximum expansion is 0.14% (Mix R4), 0.25% (Mix R3) and 0.33% (Mix R2). The specimens prepared with the Mix A of Ahmed and the Mix B of Swamy show a similar expansive behavior, the maximum expansion values are 0.7% and 0.6%, respectively. The most expansive mix is the Mix B of Ahmed (2.7%). A similar trend is observed in the degradation of the Young's modulus (Figure 2 (b)); the higher is the maximum swelling, the higher is the loss of stiffness.

Figure 2 (c), (d) and (e) present the direct and splitting tensile strength as well as the modulus of rupture (MOR) as functions of the expansion. These curves show an initial gain, which could be ascribed to the concrete hardening phenomenon.

The compressive strength is less affected by ASR than the Young's modulus and the tensile strength (Figure 2 (f)). In some cases, Mix R3 of Giaccio and Mix A of Ahmed, it increases with the expansion. According to Swamy et al. it is possible to affirm that: "compressive strength is not a good indicator of initiation or progress of ASR, particularly at early ages" [10].

#### 4. DEGRADATION MODEL FOR STIFFNESS AND TENSILE STRENGTH

The main scope of this paper is to model the anisotropic swelling behavior assuming a smeared crack model in which the concrete is considered formed by a skeleton whose pores are filled by the expansive gel. According with experimental data shown in Chapter 3, the degradation of the stiffness and the tensile strength is defined for a 1D model.

Two normalized values for the Young's modulus,  $E^*$ , and for the tensile strength,  $f_t^*$ , are defined. They are the ratio between the current value ( $E, f$ ), and their initial value evaluated at 28-days ( $E_0, f_{t0}$ ), thus:

$$E^* = E/E_0 \quad (1)$$

$$f_t^* = f_t/f_{t0} \quad (2)$$

In Figure 3 (a) the variation of the normalized stiffness in function of the swelling and the reaction extent coefficient are presented. The reaction extent coefficient is the ratio between the current expansion value,  $\varepsilon_{ASR}$ , and its maximum value,  $\varepsilon_\infty$ :

$$\xi = \varepsilon_{ASR} / \varepsilon_\infty \quad (3)$$

This coefficient varies between 0, when the reaction is not started yet, and 1, when the reaction is finished. Observing the Figure 3, it is possible to say that:

- The ASR swelling does not provoke a complete degradation of the stiffness;
- The lower is the maximum expansion value, the lower is the residual fractional stiffness (defined for  $\xi=1$ ).

In Figure 4 the variation of the normalized strength value,  $f_t^*$ , is given as a function of the swelling and the reaction extent coefficient,  $\xi$ . It is possible to observe that:

- The higher is the maximum expansion value, the higher is the initial delay in the degradation;
- The residual fractional strength (defined for  $\xi=1$ ) varies between 0.5 and 0.65.

In Figure 5 the two normalized values are shown as a function of the ratio between the current expansion,  $\varepsilon_{ASR}$ , and a characteristic strain of the concrete skeleton,  $\varepsilon_\sigma$  (Eq. (4)). The cracking strain,  $\varepsilon_\sigma = f_{t0}/E_0$ , denotes the onset of cracking in the case of external loading.

$$\chi = \varepsilon_{ASR} / \varepsilon_\sigma \quad (4)$$

In a sound concrete, when the strain reaches the critical value  $\varepsilon_\sigma$ , that is  $\chi=1$ , a sharp decrease of the stiffness and a softening behavior for the tensile stress are shown (dashed curves in Figure 5). If the concrete is affected by ASR swelling a less sharp degradation as well as the presence of a residual capacity of the material is observed (Figure 5). Therefore, the model should be able to describe the different behavior for the two damage sources, mechanical loading and ASR swelling.

Observing the experimental results of Ahmed for the Mix B, the most expansive one, some observations have been highlighted in Figure 6 (a). The stiffness degradation due to ASR swelling can be divided in three phases. At the beginning no degradation occurs until the normalized expansion strain  $\chi$  reaches the value  $\chi^I (>1)$ . Afterwards the stiffness of the system decreases until the normalized strain reaches the value  $\chi^{II}$ . In the third phase the reaction is still active, but the stiffness is constant and its residual fractional value is equal to  $E_{II}^*$ . Therefore, in order to link the stiffness degradation and the ASR expansion,

excluding any other mechanical load, three material parameters are needed: the strains which identify the beginning,  $\varepsilon_{ASR}^I$ , and the end,  $\varepsilon_{ASR}^{II}$ , of the deterioration (which correspond to the normalized value  $\chi^I$  and  $\chi^{II}$ , respectively) and the residual fraction value  $E_{II}^*$ . There is a lack of information on these parameters.

In order to model the behavior of concrete subjected to a mechanical load and to ASR swelling, the model in Figure 6 (b) is proposed. It is assumed that the concrete is a porous material in which the gel is seen as an internal expansive source. The concrete skeleton can be subjected to external (mechanical load) and internal (ASR swelling) damages. Moreover, two different degradation trends are modeled on the basis of the two damage sources, but based on the same material properties. The model should be in agreement with the known law for the sound concrete and it should also catch the observed behavior in case of ASR swelling.

The model is formed by three branches, two placed in parallel and the third one in series with the previous two. Its formulation is based on the total strain  $\varepsilon$  and the linear expansive strain due to swelling  $\varepsilon_{ASR}$ . This last one is defined through the Larive's kinetic law [3] taking in account the swelling redistribution due to the stress state, as proposed by Saouma and Perotti [6].

In order to consider the initial delay of the stiffness degradation, the imposed strain generated by the ASR swelling,  $\varepsilon_{ASR}$ , are modeled through two stress-free expansive cells in the first and third branch: the first one,  $\varepsilon_{im}$ , results in internal stresses and possible damage; instead, the second one,  $\varepsilon_{ij}$ , does not provoke damage. They are equal to:

$$\varepsilon_{im} = \alpha \varepsilon_{ASR} \quad (5)$$

$$\varepsilon_{ij} = (1 - \alpha + \gamma) \varepsilon_{ASR} \quad (6)$$

where  $\alpha$  is a distribution constant and  $\gamma$  is introduced to compensate that not all imposed strain leads to an overall strain  $\varepsilon$ . The strain  $\varepsilon_m$  is the result of the combination of mechanical loading and ASR swelling:

$$\varepsilon_m = \varepsilon - (1 + \gamma) \varepsilon_{ASR} \quad (7)$$

In the first and second branch two springs, with stiffness  $K_1$  and  $K_2$  respectively, are placed in a parallel. The two stiffness are degraded, by the damage cells placed in series with them, in agreement with the tension softening law, characterized by the parameters  $\varepsilon_{cr}$  and  $\varepsilon_u$ . The ultimate strain  $\varepsilon_u$  is the strain level where the material is completely softened in the case of pure mechanical loading. Its definition is based on regularized fracture energy.

The global stress-strain relationship is defined as:

$$\sigma = E \left( \varepsilon - \varepsilon_{ij} - \frac{(1 - d_1) K_1}{(1 - d_1) K_1 + (1 - d_2) K_2} \varepsilon_{im} \right) = E \left[ \varepsilon - \left( 1 + \gamma - \frac{(1 - d_2) K_2}{(1 - d_1) K_1 + (1 - d_2) K_2} \alpha \right) \varepsilon_{ASR} \right] \quad (8)$$

where the damage coefficients  $d_1$  and  $d_2$  are defined by the maximum value (occurred during the load history) of the strains  $\varepsilon_{im}$  and  $\varepsilon_d$ , respectively. They increase between 0 and 1 and their relationship is defined in agreement with the tension softening law. The overall stiffness  $E$  is defined by Eq. (9):

$$E = (1 - d_1) K_1 + (1 - d_2) K_2 \quad (9)$$

If the sound concrete is subjected to mechanical load, the model degenerate in an equivalent system in which a single spring, with initial stiffness equal to  $E_0$ , is placed in series with a damage cell. The degradation is governed by a single damage parameter  $d$ , which is a function of the total strain  $\varepsilon$ .

If ASR-affected concrete is in a free expansion condition, the first and second branch are in equilibrium and the total stress is equal to zero; therefore the variable  $\gamma$  is defined as:

$$\gamma = \frac{(1-d_2)K_2}{(1-d_1)K_1 + (1-d_2)K_2} \alpha \quad (10)$$

Moreover, in free expansion condition, the spring in the first branch does not result in damage ( $d_1=0$ ) because is in compression due to the ASR imposed strain  $\varepsilon_{im}$ .

In order to define the model parameters,  $K_1$ ,  $K_2$  and  $\alpha$  (Eq. (11)), the model is calibrated considering two main situation: sound concrete subjected to mechanical load and ASR-affected concrete under free expansion condition [13].

$$\left\{ \begin{array}{l} K_1 = \frac{\varepsilon_{ASR}^{II} \varepsilon_{\sigma}}{\varepsilon_{ASR}^I \varepsilon_{\mu}} E_0 \\ K_2 = E_0 - K_1 \\ \alpha = \frac{\varepsilon_{\mu}}{\varepsilon_{ASR}^{II}} \end{array} \right. \quad (11)$$

As shown in Eq. (11), the involved material parameters of the model are: the strain which defines the beginning,  $\varepsilon_{\sigma}$  and  $\varepsilon_{ASR}^I$ , and the end,  $\varepsilon_{\mu}$  and  $\varepsilon_{ASR}^{II}$ , of the degradation in case of mechanical load and free ASR swelling, respectively, and the initial overall stiffness of the system,  $E_0$ .

The degradation of the strength is derived from the adopted stress-strain relationship and the degraded stiffness value,  $E$ .

## 5. CONCLUSIONS

In this paper a literature review of the main available structural models is reported. The anisotropic aspects of ASR swelling and its important role in the modeling are underlined. According with experimental results, the ‘‘intrinsic anisotropy’’ and the ‘‘expansion transfer’’ concept are discussed.

The majority of literature models are damage model in which the expansion is characterized anisotropically through weight coefficients, as proposed by Multon et al. [5] and Saouma and Perotti [6], or orthotropically, as proposed by Capra and Sallier [8].

According with Farage et al. [9], a 1D smeared crack model approach is presented. The concrete is considered as a porous material in which the solid skeleton and the ASR gel filling the pores are characterized as a homogenized material with overall mechanical properties.

The degradation of the engineering properties is evaluated in accordance with the experimental tests by Larive [3], Swamy et al. [10], Ahmed et al. [11] and Giaccio et al. [12]. The attention is focused on the evaluation of the Young’s modulus and the tensile strength. A clear contrast to the known stress-strain degradation laws for ordinary concrete is underlined: swelling leads to a decrease of stiffness and strength, but at a substantially higher strain level, and cannot completely deteriorate the system. Additional material parameters are used to define the degradation of the Young’s modulus under the free ASR swelling. However, due to the lack of information, at this moment it is not possible to define these properties as a

function of the adopted mix. The strength degradation is defined as the combination of the degraded stiffness and the tension softening law.

### **Acknowledgements**

The authors gratefully acknowledge the financial support of the Dutch Technology Foundation STW.

### **References**

- [1] Léger, P, Côté, P, Tinawi, R (1996): Finite element analysis of concrete swelling due to alkali-aggregate reactions in dams. *Computers & Structures*, (60): 601–611.
- [2] Pietruszczak, S (1996): On the Mechanical Behaviour of Concrete Subjected to Alkali-Aggregate Reaction. *Computers & Structures*, (58.6): 1093-1097.
- [3] Larive, C (1998): Apports combinés de l'expérimentation et de la modélisation à la compréhension de l'alcali-réaction et de ses effets mécaniques. Monograph LPC, Laboratoires des Ponts et Chaussées, Paris.
- [4] Ulm, FJ, Coussy, O, Kefei, L, Larive, C (2000): Thermo-chemo-mechanics of ASR expansion in concrete structures. *ASCE Journal of Engineering Mechanics* (126.3): 233-242.
- [5] Multon, S, Toutlemonde, F (2006): Effect of applied stresses on alkali-silica reaction-induced expansions. *Cement and Concrete Research*, (36): 912–920.
- [6] Saouma, V, Perotti, L (2006): Constitutive model for alkali-aggregate reaction. *ACI Material Journal*, (103.3): 194–202.
- [7] Comi, C., Fedele, R., Perego, U., (2009): A chemo-thermo-damage model for the analysis of concrete dams affected by alkali-silica reaction. *Mechanics of Materials*, (41): 210-230.
- [8] Capra, B, Sellier, A, (2003): Orthotropic modelling of alkali-aggregate reaction in concrete structures: numerical simulations. *Mechanics of Materials*, (35): 817–830.
- [9] Farage MCR, Alves JLD, Faibairn EMR (2004): Macroscopic model of concrete subjected to alkali-aggregate reaction. *Cement and Concrete Research*, (34.3): 495-505.
- [10] Swamy, RN, Al-Asali, MM (1987): Engineering properties of concrete affected by alkali-silica reaction. *ACI Material Journal*, (85): 367–369.
- [11] Ahmed, T, Burley, E, Rigden, S, Abu-Tarir, AI (2003): The effect of alkali reactivity on the mechanical properties of concrete. *Construction and Building Materials*, (17): 123-144.
- [12] Giaccio, G, Zerbino, R, Ponce, JM, Batic, OR (2008): Mechanical behavior of concretes damaged by alkali-silica reaction. *Cement and Concrete Research*, (38): 993-1004.
- [13] Esposito, R., Hendriks, M.A.N., (2012): Degradation of the mechanical properties in ASR-affected concrete: overview and modelling. Submitted for publication in the proceeding of SSCS'12 (Strategies for Sustainable Concrete Structures), 29May-1June 2012, Aix-en-Provence, France

Test / Author	Curing and Storage Condition	Coarse aggregate		Fine Aggregate	
		Reactive	Non Reactive	Reactive	Non Reactive
Mix A Abmed [11]	28 days in water at 20°C 337 day in water at 38°C		10 mm limestone	Thames Valley sand	2 mm crushed limestone
Mix B Abmed [11]	28 days in water at 20°C 337 day in water at 38°C		10 e 20 mm limestone	Thames Valley sand and fused silica (15% *)	2 mm crushed limestone
Larive [3]	14 days in aluminum foils at 23°C 386 days in high humidity at 38°C	Siliceous limestone	Limestone	Tournaisis sand	
Mix A Swamy et al. [10]	365 days at 23°C and RH = 96 %		10 mm rounded and crushed gravel	Beltane opal (4.5% *)	Natural sand
Mix B Swamy et al. [10]	365 days at 23°C and RH = 96 %		10 mm rounded and crushed gravel	Fused silica (15% *)	Natural sand
Mix R2 Giaccio et al. [12]	1 day in cotton sheet at 21°C 745 days in water at 38°C		Granitic crushed stone	Natural sand	
Mix R3 Giaccio et al. [12]	1 day in cotton sheet at 21°C and 745 days in water at 38°C	Siliceous orthoquartzite (10% *)	Granitic crushed stone (90% *)		Natural sand
Mix R4 Giaccio et al. [12]	1 day in cotton sheet at 21°C and 745 days in water at 38°C		Slow reactive granitic crushed stone		Natural sand

\* Volume percentage of total aggregate

Test / Author	Specimens dimension [mm]					
	Expansion	Young's modulus	Direct tensile strength	Splitting tensile strength	Modulus of rupture	Compressive strength
Mix A, B Abmed [11]	100x100x500* 150x300†	150x300†	dumb-bell briquette test	100x100†	100x100x500*	100x100x100‡
Larive [3]	130x240†	130x240†	-	130x240† <sup>1</sup>	-	130x240† <sup>1</sup>
Mix A, B Swamy et al. [10]	75x75x300*	-	-	100x200† <sup>2</sup>	-	100x100x100‡
Mix R2, R3, R4 Giaccio et al. [12]	75x75x300*	100x200† 150x300†	-	-	-	100x200† 150x300†

\* Prism specimens, † Cylinder specimens, ‡ Cube specimens,  
<sup>1</sup> Average values, <sup>2</sup> Available only for Mix B

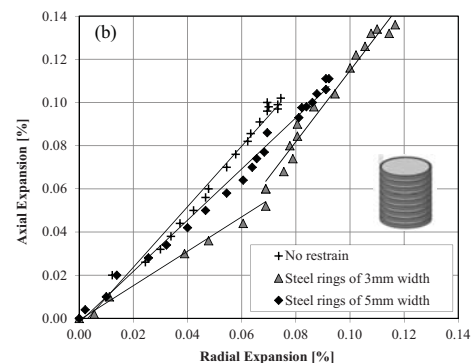
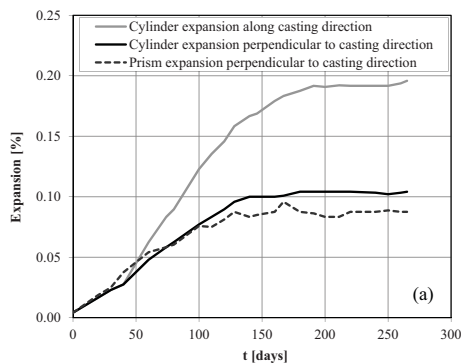


FIGURE 1: (a) Expansion curves for cylinders specimens and prisms specimens in free expansion condition [3], (b) expansions for specimens subjected to compressive load [5].

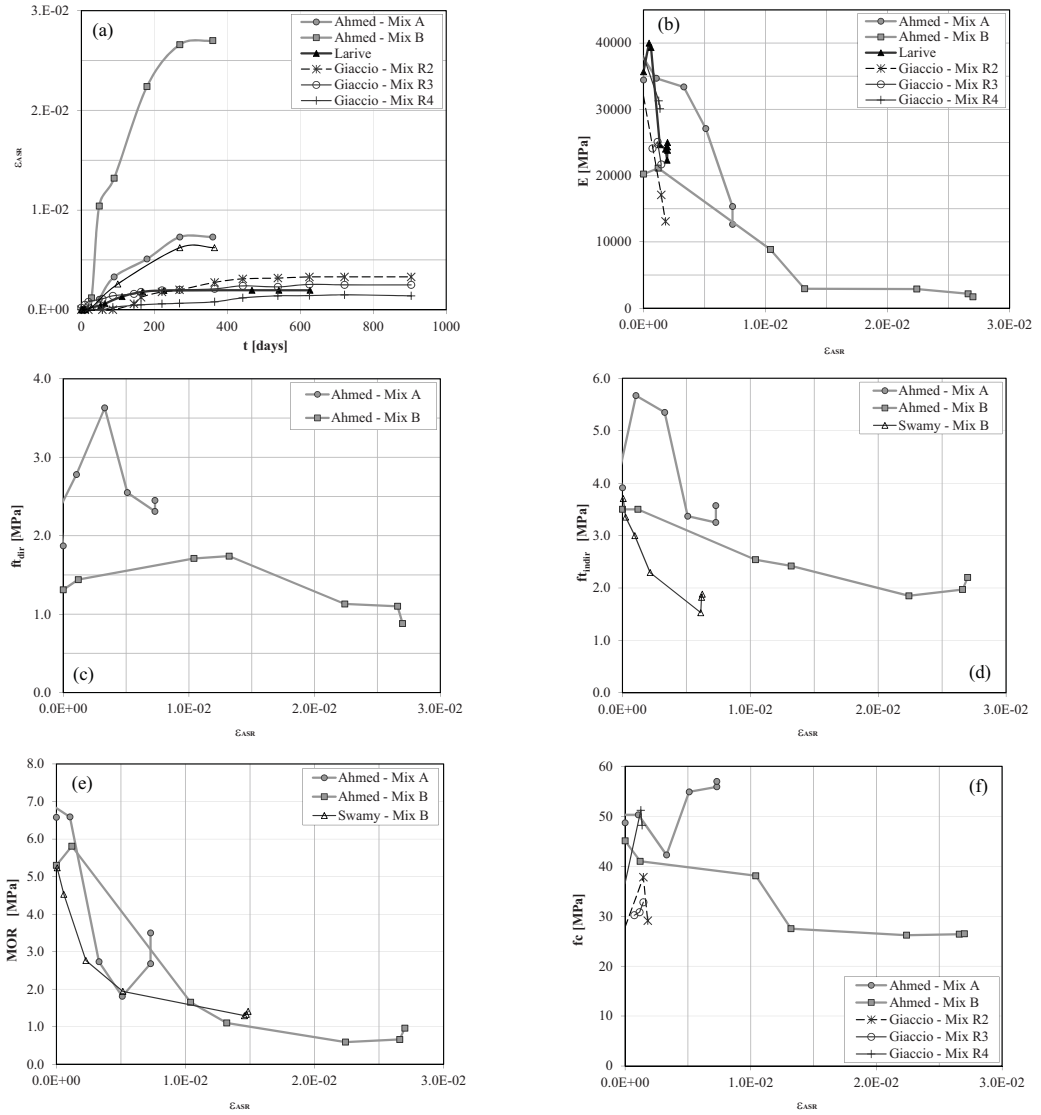


FIGURE 2: (a) Expansion vs. time curves; degradation of stiffness (b), direct (c) and splitting (d) tensile strength, MOR (e) and compressive strength (f) as a function of the swelling.

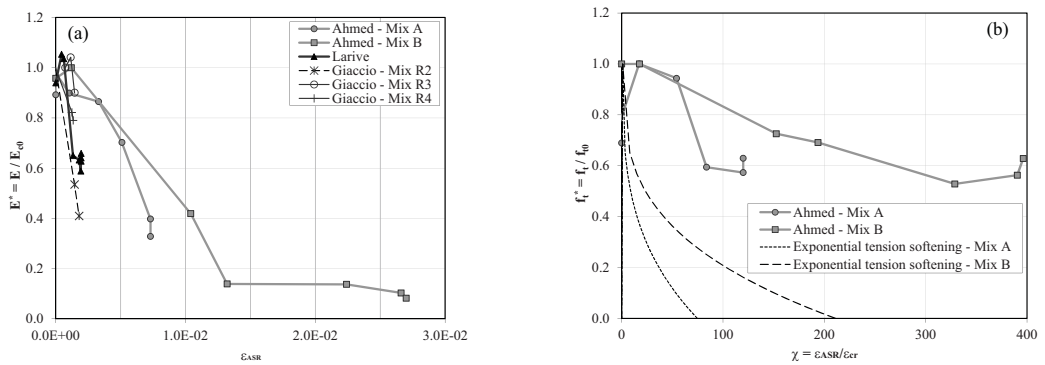


FIGURE 3: Degradation of stiffness as a function of the expansion (a) and the reaction extent (b).

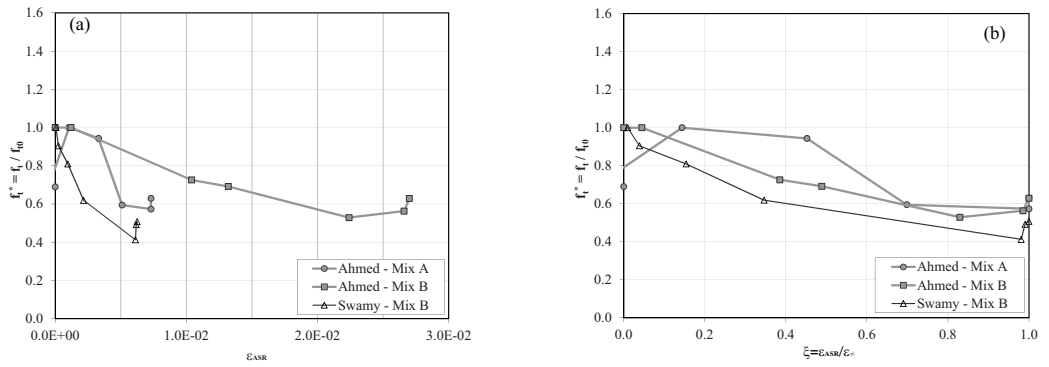


FIGURE 4: Degradation of tensile strength as a function of the expansion (a) and the reaction extent (b).

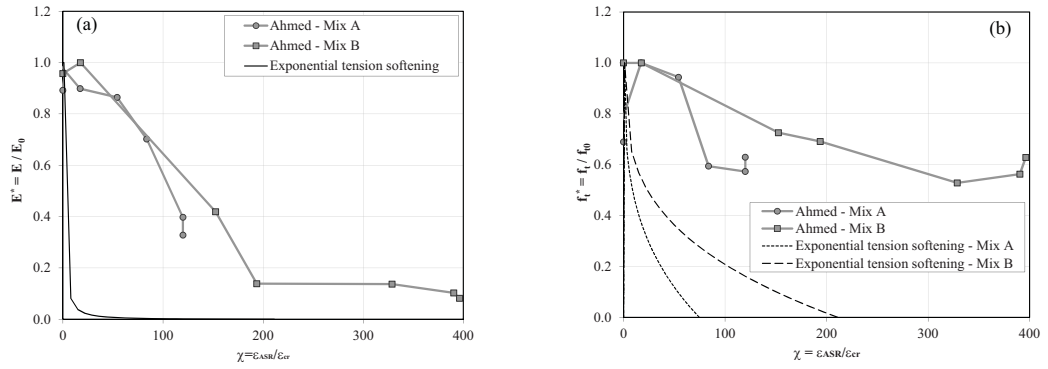


FIGURE 5: Degradation behavior for ASR-affected concrete and sound concrete.

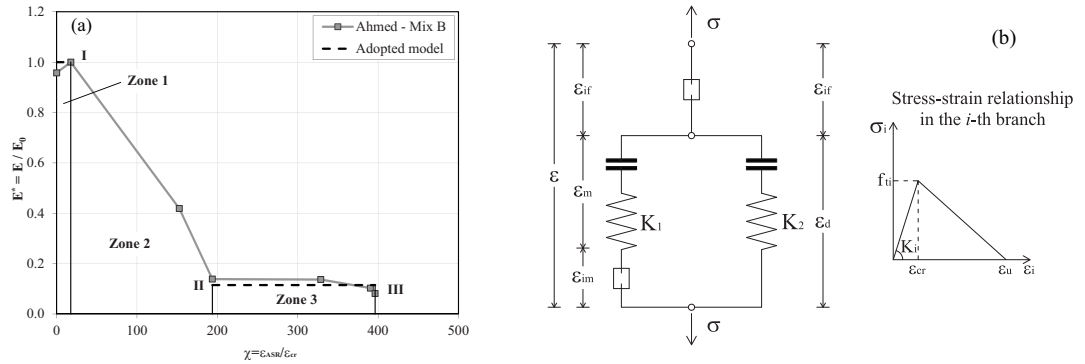


FIGURE 6: (a) Degradation model for Young's modulus; (b) Proposed 1D model smeared crack model.